Achilles' heel of iron-based catalysts during oxygen reduction in acidic medium

Chang Hyuck Choi[1]*, Hyung-Kyu Lim[2], Gajeon Chon[1], Min Wook Chung[1], Abdulrahman Altin[3], Nastaran Ranjbar Sahraie[4], Moulay-Tahar Sougrati[4], Lorenzo Stievano[4], Hyun Seok Oh[5], Eun Soo Park[5], Fang Luo[6], Peter Strasser[6], Goran Dražić[7], Karl J. J. Mayrhofer[3,8,9], Hyungjun Kim[2]* & Frédéric Jaouen[4]*

[1]School of Materials Science and Engineering, Gwangju Institute of Science and Technology, 61005 Gwangju, Republic of Korea.

[2]Department of Chemistry, Graduate School of EEWS, Korea Advanced Institute of Science and Technology, 34141 Daejeon, Republic of Korea.

[3]Department of Interface Chemistry and Surface Engineering, Max-Planck Institut für Eisenforschung GmbH, Max-Planck-Str. 1, 40237 Düsseldorf, Germany.

[4]Institut Charles Gerhardt Montpellier, UMR CNRS 5253, Agrégats, Interfaces et Matériaux pour l'Energie, Université de Montpellier, 34095 Montpellier Cedex 5, France.

[5]Department of Materials Science and Engineering, Seoul National University, 08826 Seoul, Republic of Korea.

[6]Department of Chemistry, Chemical Engineering Division, Technical University Berlin, 10623 Berlin, Germany.

[7]Department of Materials Chemistry, National Institute of Chemistry, Hajdrihova 19, 1001 Ljubljana, Slovenia.

[8]Helmholtz-Institute Erlangen-Nürnberg for Renewable Energy (IEK-11), Forschungszentrum Jülich, Egerlandstr. 3, 91058 Erlangen, Germany.

[9]Department of Chemical and Biological Engineering, Friedrich-Alexander-Universität Erlangen-Nürnberg, Egerlandstr. 3, 91058 Erlangen, Germany.

*Correspondence to: Chang Hyuck Choi (chchoi@gist.ac.kr), Hyungjun Kim (linus16@kaist.ac.kr) or Frédéric Jaouen (frederic.jaouen@umontpellier.fr)

Introduction

Fuel cells efficiently convert chemical into electric energy, with promising application for clean transportation. In proton-exchange membrane fuel cells (PEMFCs), rare platinum metal catalyzes today the oxygen reduction reaction (ORR)[1] while iron(cobalt)-nitrogen-carbon materials (Fe(Co)-N-C) are a promising alternative[2-5]. Their active sites can be classified as atomically dispersed metal-ions coordinated to nitrogen atoms (MeN_xC_y moieties)[6-9] or nitrogen functionalities (possibly influenced by sub-surface metallic particles)[10,11]. While their durability is a recognized challenge, its rational improvement is impeded by insufficient understanding of *operando* degradation mechanisms[12-18]. Here, we show that FeN_xC_y moieties in a representative Fe-N-C catalyst are structurally stable but electrochemically unstable when exposed in acidic medium to H_2O_2, the main ORR byproduct. We reveal that exposure to H_2O_2 leaves iron-based catalytic sites untouched but decreases their turnover frequency (TOF) *via* oxidation of the carbon surface, leading to weakened O_2 binding on iron-based sites. Their TOF is recovered upon electrochemical reduction of the carbon surface, demonstrating the proposed deactivation mechanism. Our results reveal a hitherto unsuspected deactivation mechanism during ORR in acidic medium. This study identifies the N-doped carbon surface as Achilles' heel during ORR catalysis in PEMFCs. Observed in acidic but not in alkaline electrolyte, these insights suggest that durable iron-nitrogen-carbon catalysts are within reach for PEMFCs if rational strategies minimizing the amount of H_2O_2 or reactive oxygen species (ROS) produced during ORR are developed.

Results and discussion

A representative Fe-N-C catalyst was selected (labelled FeNC-1), comprising Fe mainly as metal ions atomically dispersed as FeN_xC_y moieties (Fig. S1 and Table S1). These moieties are ubiquitous in Fe-N-C materials that efficiently catalyze ORR in acidic medium[7,8,13-16]. From surface-specific CO-chemisorption[19] and bulk Fe-content measurements, we determined that ≥20 % of all Fe atoms in FeNC-1 are on the surface (Fig. S1d, e). We previously demonstrated in acidic electrolyte that FeNC-1 fully retained its ORR activity after extensive cycling from 0.0 to 1.0 V_{RHE}[16], and that FeN_xC_y moieties did not leach out during electrochemical cycling[15]. In spite of this, FeNC-1 shows a continuous deactivation during steady-state operation in PEMFCs[15], a conundrum impeding the rational development of stable Fe-N-C cathodes. Partially unveiling this conundrum, H_2O_2 was shown to chemically react with Fe-N-C[14], decreasing its ORR activity, however *via* an unexplained mechanism. Here, we reveal the detailed deactivation mechanism by H_2O_2.

The ORR activity and selectivity of pristine FeNC-1 were measured in acidic and alkaline electrolytes. FeNC-1 shows a higher ORR activity in alkaline than acidic medium (Fig. 1a, b and Fig. S2), typical for Fe-N-C materials[20]. Less than 5 % hydrogen peroxide is detected above 0.3 V_{RHE} during ORR in both electrolytes (Fig. 1c, d). Changes in activity and selectivity induced by H_2O_2-treatments were then investigated. The catalytic layer comprising FeNC-1 and Nafion® ionomer was immersed in a 5 wt% H_2O_2 solution of pH 1 at 20 (label FeNC-1-20), 50 or 70 °C. The ORR activity of H_2O_2-treated FeNC-1 electrodes was then measured either in 0.1 M $HClO_4$ or KOH. During this treatment, H_2O_2 is the sole deactivating agent, a pH 1 solution without H_2O_2 not impacting the activity[15]. As seen in Fig. 1a, the ORR activity measured at pH 1 after the acidic H_2O_2-treatment decreases with increasing treatment

temperature. This drop is independent of the electrochemical potential applied to FeNC-1 during H_2O_2-treatment (Fig. S3a-c), indicating that chemical reactions between FeNC-1 and H_2O_2 must account for the activity decay. The ORR rate-determining step (RDS) is however unchanged, as revealed by similar Tafel slope (TS) of 63-67 mV dec^{-1}, except after the 70 °C H_2O_2-treatment, for which the TS-value is 110 mV dec^{-1} (Fig. 1a). The increase from 63 to 110 mV dec^{-1} might be interpreted as the RDS changing from a chemical step between the first and second electron transfer (ET) to the first ET (Fig. S4a). Regarding selectivity, increased temperature during H_2O_2-treatment continuously increases the amount of H_2O_2 released during ORR from 4 to 29 % at 0.5 V_{RHE} (Fig. 1c). Similar trends are observed for ORR activity and selectivity in alkaline electrolyte, following acidic H_2O_2-treatments (Fig. 1b, d). In contrast, peroxide-treatment in 0.1 M KOH did not modify the ORR activity nor selectivity of FeNC-1, measured either in 0.1 M $HClO_4$ or KOH (Fig. S3g, h). This strongly suggests that ROS formation from peroxide and Fe-N-C is pH-dependent, in line with the acidic pH-range chosen for producing ROS from H_2O_2 and Fe cations in the frame of environmental water remediation[21]. To demonstrate that ROS species formed during the acidic H_2O_2 treatment of Fe-N-C, we used a nitrone spin-trap (5,5-dimethyl-1-pyrroline N-oxide, DMPO) and electron paramagnetic resonance (EPR). EPR spectra of filtered solution aliquots collected after 5 min of reaction between FeNC-0.5 (prepared as FeNC-1 but with halved Fe content, comprising only FeN_xC_y moieties, see later) and H_2O_2 in DMPO identify the presence of a main signal that can be unambiguously assigned to the ·DMPO-OH spin adduct (quartet signal with 1:2:2:1 intensity ratio), observed in pH 1 but not in pH 13 conditions (Fig. S5). Other ROS than hydroxyl radicals may however have been be produced during the peroxide treatment of FeNC-0.5, since other DMPO-ROS adducts than ·DMPO-OH have a shorter lifetime and quickly

breakdown to ·DMPO-OH adducts. In summary, the spin-trap experiments further support ROS formation only in acidic environment, not in alkaline environment.

The structure and chemistry of acidic H_2O_2-treated catalysts were then investigated. As reported by us for another H_2O_2 protocol[14], the Fe K-edge extended X-ray absorption fine structure (EXAFS) spectra are unmodified by H_2O_2-treatments, indicating unmodified first-coordination sphere in FeN_xC_y moieties (Fig. 2a). EXAFS is however poorly sensitive to the second coordination sphere of FeN_xC_y moieties[8]. Mössbauer spectroscopy is more sensitive to both coordination and electron population at ^{57}Fe nuclei. The doublets D1 and D2 observed in pristine FeNC-1 (Fig. S1b) and FeNC-0.5 (prepared as FeNC-1 but with halved Fe content) are still present in H_2O_2-treated samples (Fig. S6) but the spectra have a slightly modified shape and intensity. They were analysed assuming Gaussian distributions of the quadrupole splitting (QS), justified by the structural disorder revealed by transmission electron microscopy on FeNC-1 (Fig. S1f). Such an approach reveals highest QS-probabilities in FeNC-0.5 (Fig. 2b) at the values found for doublets D1-D2 (Table S1). With increasing H_2O_2-treatment temperature, the low-QS relative intensity decreases and the distribution at high-QS is slightly modified. Such minor changes comply with modifications of the second coordination sphere in FeN_xC_y moieties, but with an intact FeN_4 core. Other possible chemical changes were investigated by X-ray photoelectron spectroscopy (XPS) and elemental analysis. The N_{1s} signal was almost unmodified after H_2O_2-treatments (Fig. 2c, Fig. S7a-d), indicating no oxidation of N-functionalities, including those ligating Fe. The total Fe and N contents were also unchanged after H_2O_2-treatment (Fig. 2e). The pore size distribution, specific surface area and bulk carbon structure of H_2O_2-treated catalysts were identical to those of FeNC-1, as revealed by N_2-physisorption (Fig. 2f) and Raman spectroscopy (not shown). The lack of modifications is

apparently contentious with decreased activity and selectivity. An important exception is the oxygen content, increasing from 5 to 10 at% (Fig. 2e). The O_{1s} signal (Fig. 2d) reveals a broad peak that was fitted with C=O (carbonyl, carboxyl) and C-O (epoxy, hydroxyl) components (Fig. S7e-h). An interesting analogy can be drawn between the oxidation process of FeNC-1 by H_2O_2 and the formation of graphene oxide (GO) from graphite, H_2O_2 and potassium ferrate[22].

These results suggest that carbon oxidation was restricted to the top-surface (without formation of volatile CO or CO_2 products), the acidic H_2O_2-treatment selectively oxidizing a fraction of surface carbon atoms *via* Fenton-like reactions with FeN_xC_y surface moieties. This might have induced a lower ORR-TOF on otherwise unmodified FeN_xC_y moieties. If this is true, the ORR-activity decrease consequential to the H_2O_2-treatment should be recovered when the carbon surface is cleaned from oxygen functionalities. We opted for electrochemical reduction to softly remove oxygen groups, a method reported for GO reduction[23]. Fig. 1e, f show that the ORR activity and selectivity in acidic medium of the H_2O_2-treated materials significantly increased after electro-reduction in 0.5 M NaCl (*e.g.* activity x3.2 for reduced FeNC-1-50). The extent of activity recovery is high for FeNC-1-20 and FeNC-1-50 (67-82 % relative to FeNC-1 activity at 0.8 V_{RHE}). Activity and selectivity recovery is however not complete, and this is amplified with highly-oxidized FeNC-1-70. This may be due to incomplete removal of oxygen groups formed during H_2O_2-treatment, especially epoxy groups as reported for electrochemically-reduced GO[23]. The possible role of metallic Fe particles in FeNC-1 on either the deactivation or activity recovery could be excluded by investigating FeNC-0.5, comprising only FeN_xC_y moieties (Fig. S6)[8]. Its ORR deactivation after H_2O_2-treatment and recovery after electro-reduction are identical to those of FeNC-1 (Fig. S3i).

We resorted to density functional theory (DFT) to understand how carbon surface oxidation modifies the TOF and selectivity of FeN_xC_y moieties. The O_2-binding energy (E_b) on FeN_4 centers, a key descriptor of ORR activity[24], and electron work function (WF) of the surface were calculated against the type, number and location of oxygen groups near FeN_xC_y moieties (Fig. S8a). The introduction of hydroxyl and especially epoxy groups in the basal plane dramatically modifies E_b from −0.59 to +0.33 eV (Fig. 3a), a conclusion valid for all oxygen adsorbates (Fig. S8b). As previously discussed by Mukerjee's group[6], electron-withdrawing groups on the carbon surface not only downshift the iron *d*-orbitals (Fig. S9), thereby decreasing iron oxophilicity (Fig. 3b), but also deplete the carbon support from π-electrons, thereby elevating the WF (Fig. 3a). Weakened E_b decreases the activity of FeNC-1, implying that FeN_4 centers integrated in graphene sheets are located either near the apex or on the weak-binding side of an activity *vs.* binding-energy volcano plot.

Selectivity toward four-electron reduction was also investigated with DFT considering the ORR mechanism detailed in Fig. 3c. The first ET results in an iron-hydroperoxo complex (step 2). If the subsequent O–OH bond cleavage and second ET occurred in a concerted step at a single FeN_xC_y moiety (step 3), a considerable reorganization energy would be expected[25]. Instead, we consider an O–O bond cleavage assisted by the nearest carbon atom, situated only 2.67 Å away from Fe (step 4, Fig. S4b), defining a cooperative OOH dissociation pathway[26]. This pathway becomes less favorable with surface oxidation (electronic effect) and could even be sterically blocked if the cooperative carbon center is occupied by an oxygen group, favoring H_2O_2 formation (Fig. S10a). Furthermore, N-doped graphene has stronger affinity to oxygen groups than graphene, inferring that surface oxidation might occur preferentially on carbons adjacent to nitrogen atoms (Fig. S10b).

Following these DFT insights, we measured WF, potential of zero charge (E_{PZC}) and basicity of H_2O_2-treated FeNC-1. Ultraviolet photoelectron spectroscopy indicates increased WF with acidic H_2O_2-treatment, leading to a negative correlation between ORR activity and WF (Fig. 4a-c). This is consistent with our DFT calculations (Fig. 3a) and recent studies on the initial ORR activity of Fe-N-C and N-S-O-C materials[27,28]. E_{PZC} is also negatively correlated with ORR activity (Fig. 4d-f). The surface basicity, pH_f, decreased with increasing H_2O_2-treatment temperature due to the acidic character of oxygen groups, leading to a positive correlation with ORR activity (Fig. 4g-i). These correlations are explained on the basis of a modulation of the TOF of FeN_xC_y moieties by the electronic properties of the surrounding carbon surface. This concept bears similarities with the importance of solid-state physics for electrochemical reaction rates, demonstrated in the 1970's for metallic surfaces[29]. In practice, in addition to decreasing the TOF of FeN_xC_y moieties *via* carbon surface oxidation, peroxide or ROS formed during PEMFC operation might also increase the catalyst's hydrophilicity and attack the proton-conductive ionomer. Both phenomena could lead to decreased transport properties through the cathode, possibly further amplifying the performance loss. For FeNC-1 however, our previous study showed that only the ORR activity significantly decreased during PEMFC operation[14].

Conclusion

In summary, we explain the main deactivation of Fe-N-C catalysts for ORR in PEMFCs as a reversible surface oxidation of carbon, decreasing the TOF of Fe-based active sites *via* weakened O_2 binding. This study provides novel insights into the *operando* deactivation of Fe-N-C catalysts comprising FeN_xC_y sites. While Fe-N-C catalysts comprising only Fe particles

encapsulated in a graphitic shell might not experience this deactivation (no surface iron), the ORR activity of such catalysts has hitherto been low[30]. The need to consider FeN_xC_y moieties in their long-range electronic and chemical environment for TOF determination and the recoverable decay of TOF are important paradigm shifts. The present study brings hope for durable Fe-N-C cathodes in high power density PEMFCs, with *in situ* (electro)reduction of carbon, H_2O_2 or radical scavengers.

Data availability

All data are available from the corresponding authors upon reasonable request.

Acknowledgements

The research leading to these results was supported by ANR under contract 2011 CHEX 004 01, by Creative Materials Discovery Program through the National Research Foundation of Korea (NRF) funded by Ministry of Science and ICT (NRF-2017M3D1A1039376) and by the European Union's Horizon 2020 research and innovation programme under grant agreement CREATE No. 721065. C.H.C. acknowledges the support by the National Research Foundation of Korea (NRF) grant funded by the Korea government (MSIP) (NRF-2017R1C1B2002918). P.S. acknowledges support by the European Commission, H2020, Fuel Cell Hydrogen Joint Undertaking (FCH-JU 2) programs.

Author contributions

C.H.C., H.K. and F.J. designed the research. G.C. and M.W.C. performed electrochemical studies. A.A., N.R.-S., M.T.S., L.S., H.S.O., E.S.P., F.L. and G.D. performed spectroscopic and other characterization measurements and analysed the data. H.-K.L. and H.K. performed computational calculations. P.S. and K.J.J.M. provided instrumental support and critical advises. C.H.C., H.K. and F.J. wrote the manuscript with comments from all authors.

Author information

Reprints and permissions information is available at www.nature.com/reprints. The authors declare no competing financial interests. Correspondence and requests for materials should be addressed to F.J. (frederic.jaouen@umontpellier.fr), H.K. (linus16@kaist.ac.kr) or C.H.C. (chchoi@gist.ac.kr).

References

1 Debe, M. K. Electrocatalyst approaches and challenges for automotive fuel cell s. *Nature* **486**, 43-51 (2012).

2 Lefèvre, M., Proietti, E., Jaouen, F. & Dodelet, J. P. Iron-based catalysts with improved oxygen reduction activity in polymer electrolyte fuel cells. *Science* **32 4**, 71-74 (2009).

3 Wu, G., More, K. L., Johnston, C. M. & Zelenay, P. High-performance electro catalysts for oxygen reduction derived from polyaniline, iron, and cobalt. *Scien ce* **332**, 443-447 (2011).

4 Li, Y. *et al.* An oxygen reduction electrocatalyst based on carbon nanotube-gra phene complexes. *Nat. Nanotechnol.* **7**, 394-400 (2012).

5 Chung, H. T. *et al.* Direct atomic-level insight into the active sites of a high-p erformance PGM-free ORR catalyst. *Science* **357**, 479-484 (2017).

6 Ramaswamy, N., Tylus, U., Jia, Q. & Mukerjee, S. Activity descriptor identific ation for oxygen reduction on nonprecious electrocatalysts: Linking surface scie nce to coordination chemistry. *J. Am. Chem. Soc.* **135**, 15443-15449 (2013).

7 Kramm, U. I. *et al.* On an easy way to prepare metal-nitrogen doped carbon with exclusive presence of MeN_4-type sites active for the ORR. *J. Am. Chem. Soc.* **138**, 635-640 (2016).

8 Zitolo, A. *et al.* Identification of catalytic sites for oxygen reduction in iron- a nd nitrogen-doped graphene materials. *Nat. Mater.* **14**, 937-942 (2015).

9 Fei, H. *et al.* Atomic cobalt on nitrogen-doped graphene for hydrogen generati on. *Nat. Commun.* **6**, 8668 (2015).

10 Gong, K., Du, F., Xia, Z., Durstock, M. & Dai, L. Nitrogen-doped carbon nan

otube arrays with high electrocatalytic activity for oxygen reduction. *Science* **323**, 760-764 (2009).

11 Guo, D. *et al.* Active sites of nitrogen-doped carbon materials for oxygen reduction reaction clarified using model catalysts. *Science* **351**, 361-365 (2016).

12 Ferrandon, M. *et al.* Stability of iron species in heat-treated polyaniline-iron-carbon polymer electrolyte fuel cell cathode catalysts. *Electrochim. Acta* **110**, 282-291 (2013).

13 Goellner, V. *et al.* Degradation of Fe/N/C catalysts upon high polarization in acid medium. *Phys. Chem. Chem. Phys.* **16**, 18454-18462 (2014).

14 Goellner, V., Armel, V., Zitolo, A., Fonda, E. & Jaouen, F. Degradation by hydrogen peroxide of metal-nitrogen-carbon catalysts for oxygen reduction. *J. Electrochem. Soc.* **162**, H403-H414 (2015).

15 Choi, C. H. *et al.* Minimizing operando demetallation of Fe-N-C electrocatalysts in acidic medium. *ACS Catal.* **6**, 3136-3146 (2016).

16 Choi, C. H. *et al.* Stability of Fe-N-C catalysts in acidic medium studied by operando spectroscopy. *Angew. Chem. Int. Ed.* **54**, 12753-12757 (2015).

17 Lefèvre, M. & Dodelet, J. P. Fe-based catalysts for the reduction of oxygen in polymer electrolyte membrane fuel cell conditions: Determination of the amount of peroxide released during electroreduction and its influence on the stability of the catalysts. *Electrochim. Acta* **48**, 2749-2760 (2003).

18 Wu, G. *et al.* Performance durability of polyaniline-derived non-precious cathode catalysts. *ECS Trans.* **25**, 1299-1311 (2009).

19 Sahraie, N. R. *et al.* Quantifying the density and utilization of active sites in non-precious metal oxygen electroreduction catalysts. *Nat. Commun.* **6**, 8618 (20

15).

20 Brocato, S., Serov, A. & Atanassov, P. pH dependence of catalytic activity for ORR of the non-PGM catalyst derived from heat-treated Fe-phenanthroline. *Ele ctrochim. Acta* **87**, 361-365 (2013).

21 Nidheesh, P. V. Heterogeneous Fenton catalysts for the abatement of organic p ollutants from aqueous solution: a review. *RSC Adv.* **5**, 40552-40577 (2015).

22 Yu, C., Wang, C. F. & Chen, S. Facile access to graphene oxide from ferro-in duced oxidation. *Sci. Rep.* **6**, 17071 (2016).

23 Guo, H. L., Wang, X. F., Qian, Q. Y., Wang, F. B. & Xia, X. H. A green a pproach to the synthesis of graphene nanosheets. *ACS Nano* **3**, 2653-2659 (200 9).

24 Zagal, J. H. & Koper, M. T. M. Reactivity descriptors for the activity of mole cular MN_4 catalysts for the oxygen reduction reaction. *Angew. Chem. Int. Ed.* **55**, 14510-14521 (2016).

25 Choi, C. H. *et al.* Tuning selectivity of electrochemical reactions by atomically dispersed platinum catalyst. *Nat. Commun.* **7**, 10922 (2016).

26 Kattel, S. & Wang, G. Reaction pathway for oxygen reduction on FeN_4 embed ded graphene. *J. Phys. Chem. Lett.* **5**, 452-456 (2014).

27 Choi, C. H. *et al.* Long-range electron transfer over graphene-based catalyst for high-performing oxygen reduction reactions: Importance of size, N-doping, and metallic impurities. *J. Am. Chem. Soc.* **136**, 9070-9077 (2014).

28 Cheon, J. Y. *et al.* Intrinsic relationship between enhanced oxygen reduction re action activity and nanoscale work function of doped carbons. *J. Am. Chem. S oc.* **136**, 8875-8878 (2014).

29 Trasatti, S. Work function, electronegativity, and electrochemical behaviour of metals: III. Electrolytic hydrogen evolution in acid solutions. *J. Electroanal. Ch em. Interfacial Electrochem.* **39**, 163-184 (1972).

30 Varnell, J. A. *et al*. Identification of carbon-encapsulated iron nanoparticles as active species in non-precious metal oxygen reduction catalysts. *Nat. Commun.* **7**, 12582 (2016).

Figures

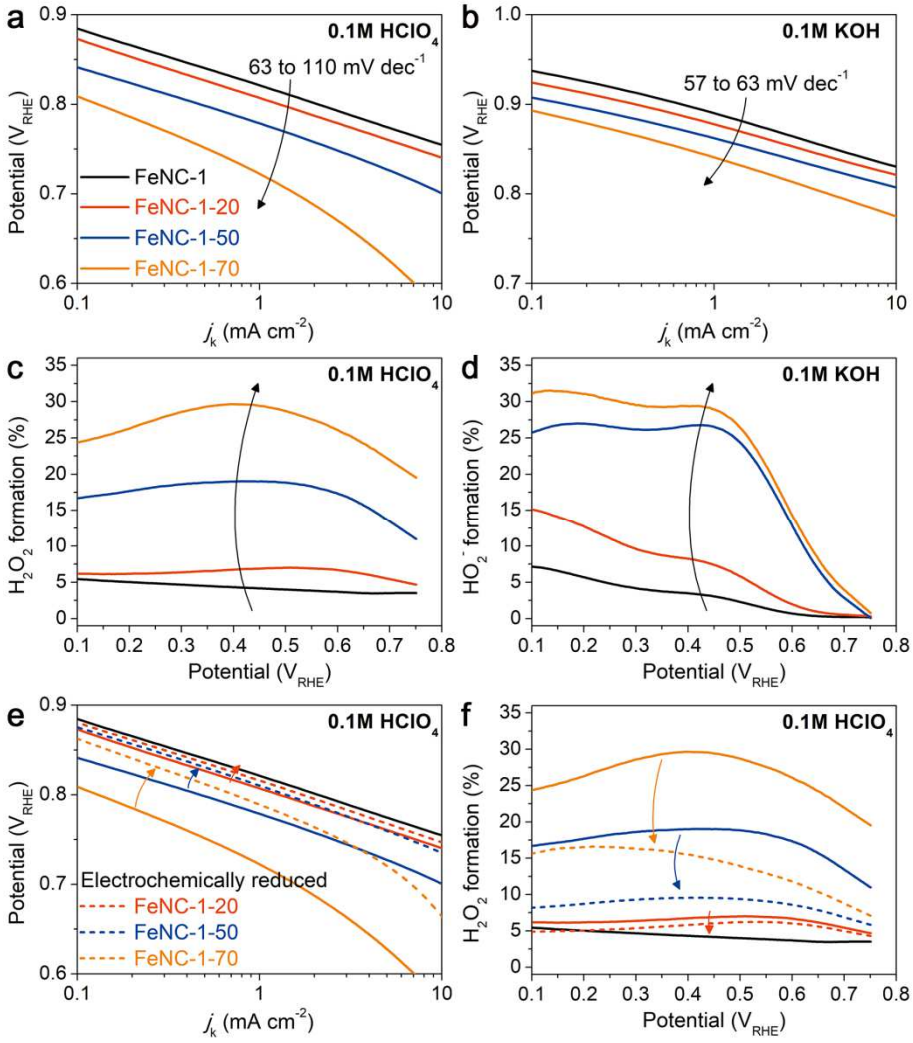

Figure 1 | Effects of acidic H_2O_2-treatment and subsequent electro-reduction in 0.5 M NaCl on the ORR activity and selectivity of FeNC-1. a, b, ORR polarization curves after 2 hour treatment at OCP (*ca.* 0.84 V_{RHE}) in 5 wt% H_2O_2 in 0.1 M $HClO_4$, **c, d,** Peroxide formation during ORR after H_2O_2-treatment, **e,** ORR polarization curves after H_2O_2-treatment and electro-reduction in 0.5 M NaCl, **f,** Peroxide formation during ORR after H_2O_2-treatment and electro-reduction in 0.5 M NaCl. The electrolyte was O_2-saturated 0.1 M $HClO_4$ (**a**, **c, e, f**) or 0.1 M KOH (**b**, **d**). The two-digit number following FeNC-1 indicates the H_2O_2-treatment temperature.

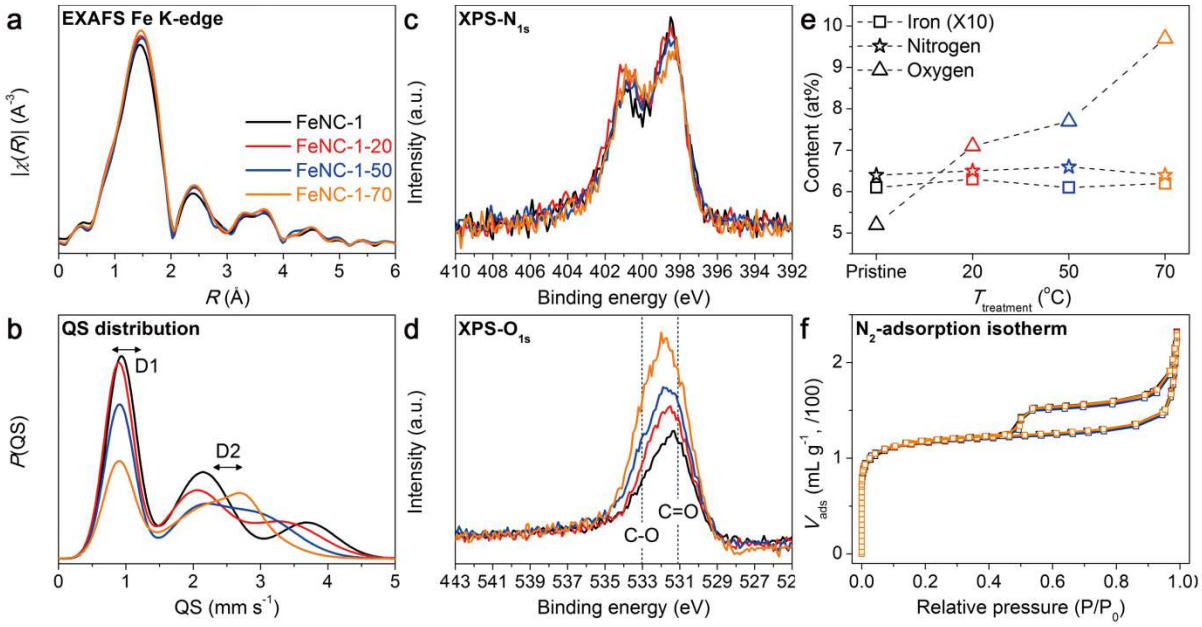

Figure 2 | Effects of acidic H_2O_2-treatment on Fe coordination, contents of iron, nitrogen, oxygen and porous structure of FeNC-1. a, k^2-weighted Fourier transforms of the Fe K-edge EXAFS spectra. **b**, ^{57}Fe Mössbauer quadrupole splitting distributions. **c**, XPS-N_{1s} spectra. **d**, XPS-O_{1s} spectra. **e**, N and O contents measured by XPS and Fe-contents measured by ICP-AES. **f**, N_2-adsorption isotherms (BET specific area and pore volume for all samples are 435 ± 5 m^2 g^{-1} and 0.35 ± 0.01 cm^3 g^{-1}, respectively). FeNC-1 was treated for 2 hours at OCP (*ca.* 0.84 V_{RHE}) in 5 wt% H_2O_2 in 0.1 M $HClO_4$ at 20, 50 or 70 °C. EXAFS, ^{57}Fe Mössbauer spectroscopy and ICP-AES are bulk techniques while XPS, probing several nm below the surface, is not a true surface-specific technique when applied to carbon materials. Note 1: Fe_{2p} signal measured with XPS was too noisy for Fe quantification. Note 2: All data were measured on FeNC-1 series, except for Mössbauer spectra (see Fig. S6). Note 3: The relative carbon content decrease that can be deduced from **Fig. 2e** results from the addition of oxygen groups on the surface, not from the irreversible loss of carbon atoms.

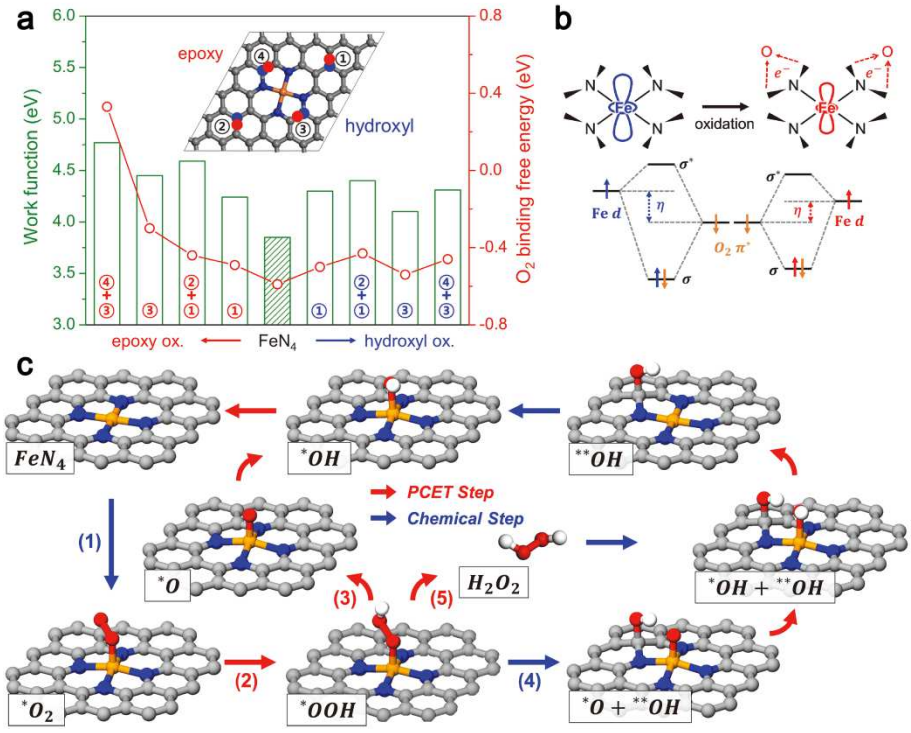

Figure 3 | First-principle DFT analysis of the effect of surface oxidation on a FeN_4 moiety embedded in a basal graphene plane. a, O_2-binding energy of FeN_4 and electron work function. The surface is either oxygen-free or oxidized with one or two oxygen-functionalities, at positions as indicated in the insets. **b**, Scheme of electron depletion at the FeN_4 center induced by surface oxidation. **c**, ORR pathways at FeN_4. Single and double asterisks denote reaction intermediates adsorbed on the Fe-center and nearest C-center, respectively.

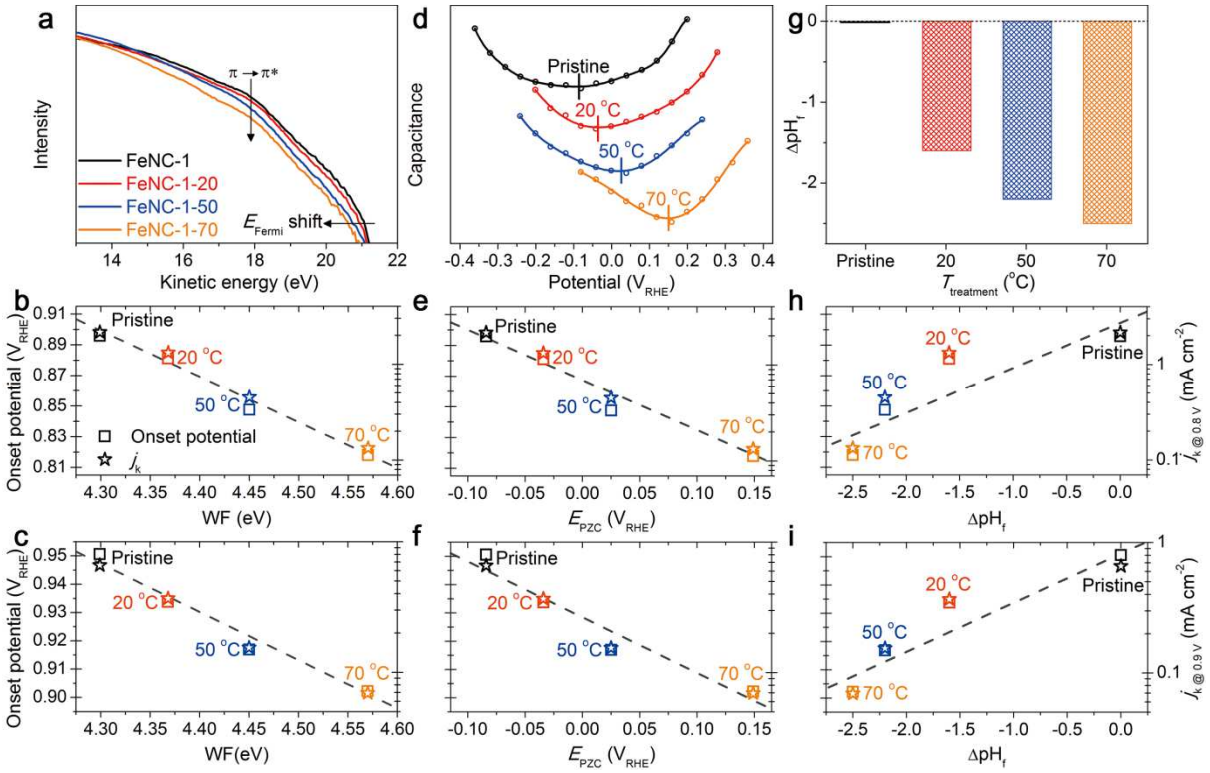

Figure 4 | Effects of acidic H_2O_2-treatment on surface properties and correlations between ORR activity and surface properties. a-c, WF, **d-f,** E_{PZC} and **g-i**, surface basicity variation (ΔpH_f). Correlations between the ORR activity in 0.1 M $HClO_4$ and WF (**b**), E_{PZC} (**e**) or ΔpH_f (**h**). Correlations between the ORR activity in 0.1 M KOH and WF (**c**), E_{PZC} (**f**) or ΔpH_f (**i**). The activity was quantified either by onset potential (left-handside axis, open square symbol) or by the kinetic current density j_k (right-handside axis, open star symbol, reported for 0.8 and 0.9 V_{RHE} in $HClO_4$ and KOH electrolytes, respectively). A logarithmic scale was used for j_k since it is logarithmically related the onset potential *via* the Tafel law.